J Supercond Nov Magn (2017) 30:1533–1538
DOI 10.1007/s10948-016-3923-2

ORIGINAL PAPER

Zinc-Blende MnTe Under Pressure: Structural, Mechanical, and Optical Properties from Ab Initio Calculation

Abdelghani Khaldi[1] · Hatem Ghodbane[2] · Nadir Bouarissa[3] · Saleh Daoud[1] · Zahir Rouabah[1] · Laurent-Tabourot[4]

Received: 14 September 2016 / Accepted: 22 November 2016 / Published online: 13 December 2016

Abstract We present first-principles studies of structural, mechanical, and optical properties of zinc blende MnTe using the pseudopotential plane-wave method within the local density approximation. The effect of hydrostatic pressure on investigated properties has been examined and discussed. At zero pressure, our results are found to agree reasonably well with those reported in the literature. The generalized elastic stability criteria showed that the material of interest is mechanically stable in all the studied pressure ranges. Applied pressure is found to shift all optical spectra under consideration, giving new optical parameters.

Keywords MnTe · Pressure · Structural properties · Mechanical properties · Optical properties · Ab initio

1 Introduction

In recent years, interest in Mn-doped IIB–VI semimagnetic semiconductors has been increased [1–6]. Manganese(II) telluride with the chemical formula MnTe is an inorganic compound. It exhibits novel electronic and magnetic properties as compared to MnO, MnS, and MnSe [7–9]. Growth methods [7, 8, 10–13] showed that the stable modification of the material of interest is the hexagonal NiAs-type structure. Nevertheless, MnTe can appear within other structures such as a cubic rock salt or NaCl structure depending on the temperature [5, 14]. Moreover, at low temperatures, it has been reported that for epitaxial MnTe layers grown by molecular beam epitaxy on cubic substrates [15–18], MnTe appeared within the metastable zinc blende phase. In this phase, the material under investigation is a magnetic semiconductor that has technological applications as a constituent of II–VI quantum structures that have been used in spintronic experiments [4].

The investigation of materials under pressure has become an important research activity. This is due to the development of the diamond anvil cell and the static pressure range extension of optical and X-ray measurements [19–21]. On the other hand, reliable computational techniques for electronic structure and ab initio calculations have given a deeper understanding of the material fundamental properties under pressure [22–27]. In fact, pressure tuning has an important effect on the fundamental properties of semiconducting materials and can lead to new materials with novel behavior properties.

In spite of the importance of zinc blende magnetic semiconductor MnTe, there have been only few works on the fundamental properties of MnTe under pressure. For that, further investigations of the material of interest under pressure are needed. In the present contribution, the pressure dependence of structural, mechanical, and optical properties for zinc blende MnTe has been studied using a pseudopotential plane-wave method as implemented in the CASTEP code [28]. The aim of the present study is to investigate the

✉ Nadir Bouarissa
n_bouarissa@yahoo.fr

[1] Laboratory of Materials and Electronic Systems (LMSE), University of Mohamed El Bachir El Ibrahimi, 34000, Bordj Bou Arreridj, Algeria

[2] Laboratoire de Modélisation des Systèmes Energétiques (LMSE), Université de Biskra, 07000, Biskra, Algeria

[3] Laboratory of Materials Physics and Its Applications, University of M'Sila, 28000, M'Sila, Algeria

[4] Laboratoire SYMME, Université Savoie Mont Blanc, 74000 Annecy, France

MnTe properties of interest in the zinc blende structure, with emphasis on their dependence on hydrostatic pressure.

2 Computational Methodology

The present calculations are carried out using a pseudopotential plane-wave method as implemented in the CASTEP code [28]. The Vanderbilt-type ultra-soft pseudopotentials [29] are used so as to represent the interactions of valence electrons with ion cores for Mn (3d5, 4S2) and Te (5S2, 5p4). The treatment of the exchange correlation potential has been made within the local density approximation (LDA) of Ceperley and Alder [30] as parameterized by Perdew and Zunger [31].

The cutoff is set as 400 eV for the planewave basis set. Brillouin zone integrations are performed using Monkhorst and Pack k-point meshes [32], with a $12 \times 12 \times 12$ special k-point mesh. These parameters are sufficient to achieve the convergence for the total energy and elastic moduli.

The optimized geometries of MnTe are determined using the Broyden-Fletcher-Goldfarb-Shanno (BFGS) minimization technique as reported in Ref. [33]. The spin polarization of the material of interest is taken into consideration. As regards the electronic minimization, the electronic occupation has been smeared using a Gaussian scheme with a smearing width of 0.1 eV.

To calculate the single-crystal elastic coefficients (C_{ij}), the finite strain-stress method [34] has been used. By deriving C_{ij}, the polycrystalline elastic parameters have been determined within the Voigt-Reuss-Hill approximation [35–38].

The convergence tolerance for the optimized geometry calculations is selected in such a way that the minimum energy, the maximum force, the maximum stress, and the maximum displacement are less than 5×10^{-6} eV/atom, 0.01 eV/Å, 0.02 GPa, and 5.0×10^{-4} Å, respectively

3 Results and Discussion

3.1 Structural Properties

The calculated relaxed lattice constant (a_0), the unit cell volume (V_0), and the inter-atomic bond length (d) for zinc blende MnTe are depicted in Table 1 which contains also the available experimental data reported in the literature to compare with our present results. Note that the discrepancy between our calculated a_0 and that reported for epitaxial MnTe layers grown by molecular beam epitaxy on cubic substrates [13, 18] is less than 2 %. The same conclusion is drawn for the unit cell volume with a deviation of less than 6 %.

Table 1 Calculated zero pressure equilibrium structural parameters for zinc blende MnTe: lattice constant (a), unit cell volume (V_0), and interatomic distance (d_0), compared to data available in the literature

Parameter	This work	Others
a_0 (Å)	6.2142	6.337 [13, 18] (Expt.)
V_0 (Å^3)	59.99	63.6196 [13, 18] (Expt.)
d_0 (Å)	2.6908	–
B_0 (GPa)	50.38	37 [4] (Expt.); 29 [4] theory
		52.67 [2][a] (Expt.); 50 [4] theory
$B\prime$	4.50	–

[a]Determined from the experimental values of the elastic constants C_{11} and C_{12} reported in Ref. [2] using the relation $B = 1/3(C_{11} + 2C_{12})$

The process of the geometry optimization is performed at various pressures. Figure 1 represents the resulting total energy-volume (E-V) data. These data are fitted to the Birch-Murnaghan equation of states [39, 40] to obtain the equilibrium bulk modulus denoted by B_0 and its pressure derivative denoted by $B\prime$. The values obtained for B_0 and $B\prime$ are given in Table 1. Also shown for comparison are the data quoted in the literature. We observe that while our calculated B_0 values disagree with the experimental value of 37 GPa reported by Djemia et al. [4] using the Brillouin light scattering, it agrees well with the experimental one of 52.67 GPa determined from the elastic constants reported by Abramof et al. [2] using reflection high-energy electron diffraction experiments. On the theoretical side, our result is much larger than that of 29 GPa calculated by Djemia et al. [4] using ab initio calculations within the generalized gradient approximation. Nevertheless, our calculated value of B_0 is in perfect agreement with that of 50 GPa calculated by the same authors of Ref. [4] using the local spin density approximation. In the absence of both theoretical and experimental

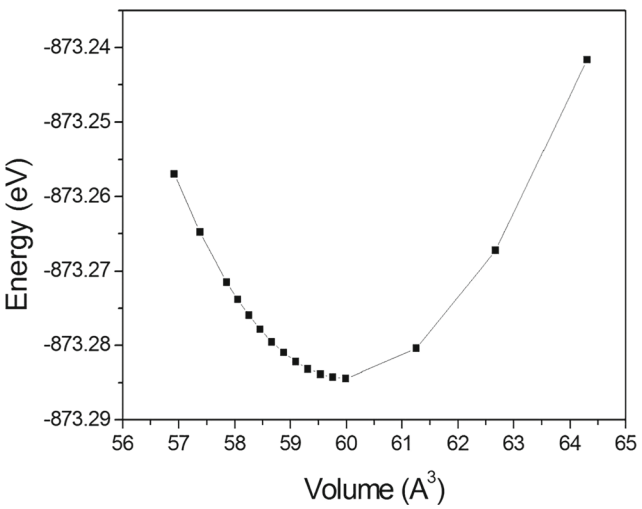

Fig. 1 Total energy versus volume for zinc blende MnTe

data concerning $B\prime$ for zinc blende MnTe, to the best of our knowledge, our result is only for reference and may save for future studies.

The response of zinc blende MnTe to external applied pressure has been estimated by exploring the dependence of the normalized lattice constant (a/a_0), bond length (d/d_0), and unit cell volume (V/V_0) on the applied hydrostatic pressure. Our results are shown in Fig. 2. Note that all normalized structural parameters decrease monotonically with raising pressure.

3.2 Mechanical Properties

Mechanical properties of semiconducting materials are very important for the understanding of many of their fundamental properties. Specifically, the elastic constants describe the response to an applied macroscopic stress and provide information about the elasticity and mechanical stability of materials. In the present contribution, the elastic constants of zinc blende MnTe have been calculated. As a matter of fact, if the crystal possesses symmetry elements, which is exactly the case of cubic crystals, the number of independent elastic constants is usually reduced. In the present case, there are only three independent stiffness constants, namely C_{11}, C_{12}, and C_{44}. The evaluated elastic constants (C_{ij}) for zinc blende MnTe at zero pressure are listed in Table 2. Also shown for comparison are the experimental findings reported in the literature. Note that the experimental values reported by Buschert et al. [17] using triple-crystal X-ray diffraction are much lower than our results and those measured by other groups [2, 4]. These values seem also to be the smallest ones as compared to those of all the other zinc blende or diamond structure materials studied so far.

Table 2 Elastic constants (C_{ij}) expressed in gigapascals of zinc blende MnTe at zero pressure

Elastic constants	This work	Others
C_{11}	59.98	50 ± 1 [4] (Expt.); 52 ± 4 [4] (Expt.)
		≈ 60 [2] (Expt.); 22.2 ± 1 [17] (Expt.)
C_{12}	46.07	31 ± 1 [4] (Expt.); ≈ 49 [2] (Expt.)
		11.6 ± 1 [17] (Expt.)
C_{44}	16.91	14.7 ± 0.3 [4] (Expt.)

However, our results appear to be in very good agreement with the experimental ones reported by Abramof et al. [2]. Moreover, the agreement between our calculated C_{11} and C_{44} and the experimental values reported by Djemia et al. [4] using both the Brillouin and Raman light scattering is reasonable.

The variation of independent elastic constants (C_{ij}) as a function of hydrostatic pressure for zinc blende MnTe is displayed in Fig. 3. Note that by raising pressure up to 4 GPa, C_{11} and C_{12} increase monotonically, exhibiting almost a linear behavior. However, C_{44} seems to decrease with increasing pressure. The behavior is monotonic and appears to be almost linear as well. Thus, the linear pressure coefficients of C_{ij} are calculated from a linear fit of C_{ij} versus pressure. Our results showed that the pressure derivatives of C_{ij}, i.e., dC_{11}/dP, dC_{12}/dP, and dC_{44}/dP, are 3.49, 4.79, and -0.99, respectively. Accordingly, one can notice that C_{44} is less sensitive to pressure than C_{11} and C_{12}.

The ductility and brittleness of semiconducting materials are two important mechanical properties that are determined directly from the elastic constants [27]. An empirical relationship between the plastic properties and elastic moduli of

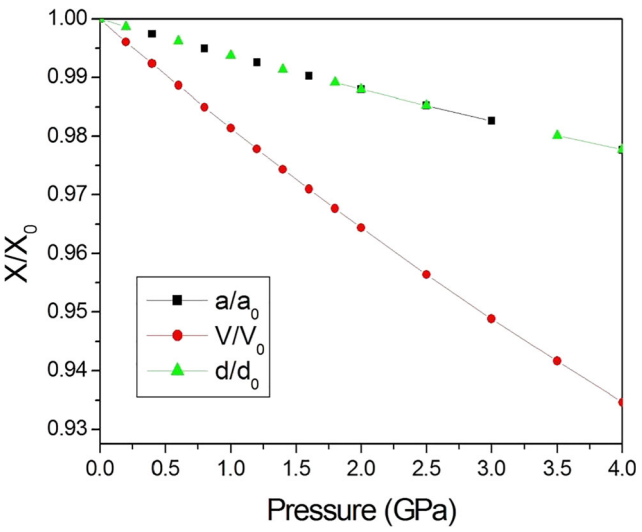

Fig. 2 Normalized lattice constant, unit cell volume, and bond length versus pressure for zinc blende MnTe

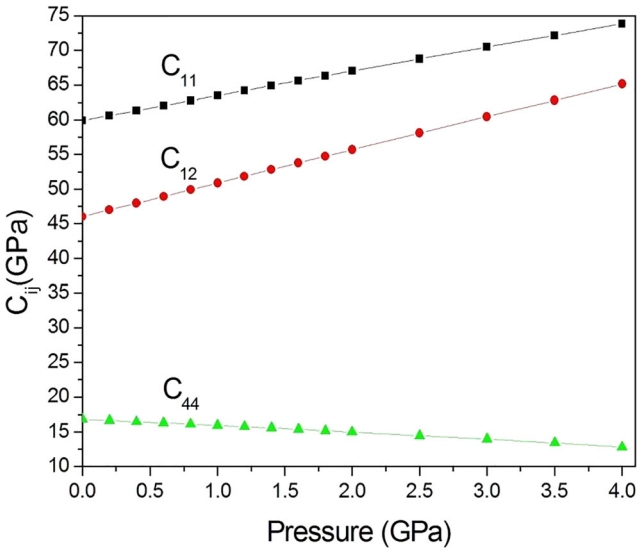

Fig. 3 Elastic constants (C_{ij}) and bulk modulus (B) versus pressure for zinc blende MnTe

semiconducting materials has been reported by Pugh [41]. To study the mechanical behavior of semiconductors, one distinguishes two thermodynamic parameters which are the Voigt averaged shear modulus referred to as G and the bulk modulus B. G represents the resistance to plastic deformation of the material, whereas B represents the resistance to fracture. Thus, if the ratio $R_{G/B}$ is greater than 0.5, the material behaves in a brittle manner; on contrary, when $R_{G/B}$ is less than 0.5, the material behaves in a ductile manner. In our case, $R_{G/B}$ is less than 0.5 which indicates that the material of interest behaves in a ductile manner.

In order to check the mechanical stability of the material under consideration, we have used the generalized elastic stability criteria as reported in Ref. [27]

$$K = \frac{1}{3}(C_{11} + 2C_{12} + P) > 0 \quad (1)$$

$$G = \frac{1}{2}(C_{11} - C_{12} - 2P) > 0 \quad (2)$$

$$G' = (C_{44} - P) > 0 \quad (3)$$

According to our results concerning C_{ij}, all stability criteria are verified for pressures in the range 0–4 GPa, thus suggesting that zinc blende MnTe is mechanically stable in the studied pressure range.

In Fig. 4, we display the generalized elastic stability criteria as a function of applied pressure. Note that as pressure increases, K increases as well. This is not the case of G and $G\prime$ which decrease monotonically with raising pressure. It is worth noting that G vanishes at about 4.23 GPa.

3.3 Optical Properties

To characterize the linear optical properties of semiconducting materials that have a cubic symmetry, one has to deal only with one dielectric tensor component. In this respect, the dielectric function imaginary part is obtained using the same methodology as that reported in Ref. [42], whereas the dielectric function real part is derived from the imaginary one using the Kramers-Kronig expression. Figure 5 shows the computed optical real and imaginary parts of the dielectric function for zinc blende MnTe at zero pressure and under pressure of 4 GPa. From an inspection of Fig. 5, one notes that the real and imaginary parts of the dielectric function exhibit almost the same qualitative behavior with some differences in details. We observe that for smaller frequencies, the curve of the real part exhibits a maximum close to the absorption edge. This maximum is followed by regions with the general tendency for reduced intensity. A similar trend has been reported by Khan and Bouarissa [43] for ZnS using ab initio molecular dynamics simulation. The applied pressure of 4 GPa seems to decrease the maximum of the main peak without affecting the shape of the peak. The decrease of the peak can be explained by the interband transitions that change under pressure. The general shape of the real part is that expected for a harmonic oscillator. The latter has a resonant frequency at around 7 eV. The applied pressure shifts the resonant frequency slightly towards higher frequencies. This is due to the change in the separation between the average bonding-anti-bonding energy level under applied hydrostatic pressure. As far as the imaginary part is concerned, one can note the presence of peaks followed by regions that are modulated by peak structures which are related to critical points in the

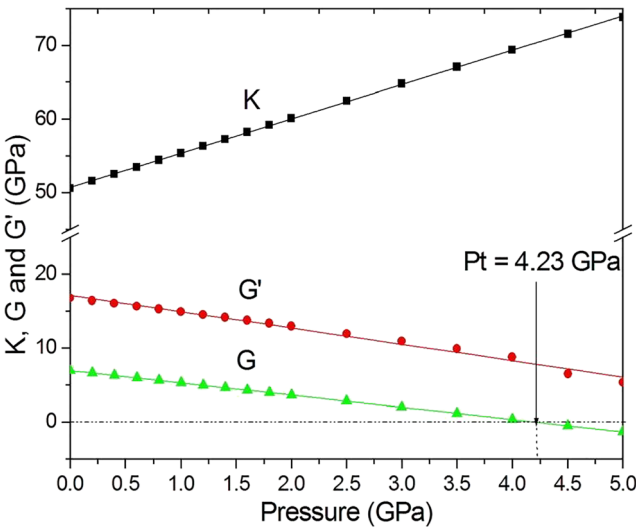

Fig. 4 Generalized elastic stability criteria, G, $G\prime$, and K, versus pressure for zinc blende MnTe

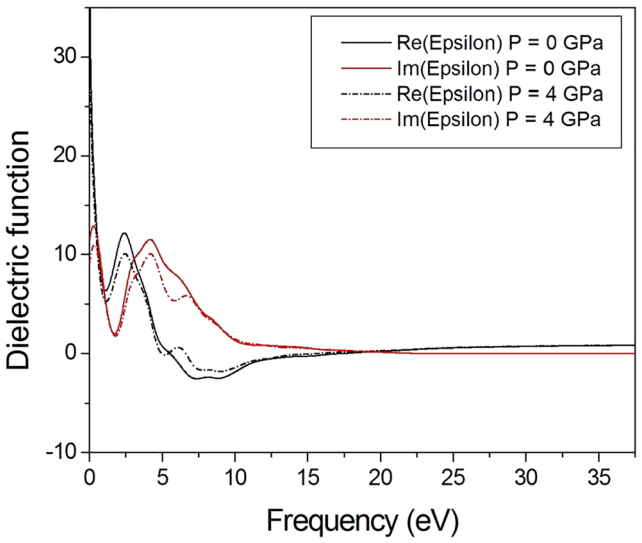

Fig. 5 Real and imaginary parts of the dielectric function for zinc blende MnTe at zero pressure and under 4 GPa pressure

Brillouin zone. The peaks are affected by pressure where their maximum is decreased. This has been accompanied by a shift of all positions of critical points with a change in energy with respect to that at zero pressure. This may be due to the change of the direct band gaps under applied pressure. Although these peaks are quantitatively affected under hydrostatic pressure, their shapes seem to remain almost similar to these at zero pressure. The decrease of the maximum of the central peak of the imaginary part of the dielectric constant with raising hydrostatic pressure is explained by the decrease of the lattice constant under pressure. The shift of the positions of the critical points under applied pressure involves a transition between valence and higher conduction bands at the Brillouin zone center and along the [111] direction.

The penetration into a material of the light of a particular wavelength before its absorption can be determined by the optical absorption coefficient. The latter has been calculated as a function of the photon energy at zero pressure and under 4 GPa pressure and is displayed in Fig. 6. Note that at zero pressure when increasing the photon energy up to about 8 eV, the optical absorption coefficient increases and then it decreases and vanishes at a photon energy of about 23 eV. When pressure is applied, the peaks of the optical absorption coefficient spectra decrease in magnitude. Nevertheless, this behavior seems to depend on the energy of light which is being absorbed.

Figure 7 shows the optical conduction of zinc blende MnTe at zero pressure and under 4 GPa pressure plotted against the photon energy. Note that the optical conduction depends strongly on the photon incident energy (wavelength). It reaches its maximum when the photon energy is in the range 5–10 eV, and it vanishes for photon energies beyond the value of about 23 eV. The applied pressure of 4 GPa leads to the decrease of the optical conductivity. The effect seems to be more important in the photon energy range 5–10 eV. The decrease of the optical conductivity under applied pressure suggests the decrease of the rate at which electrons absorb incident photons for a given energy.

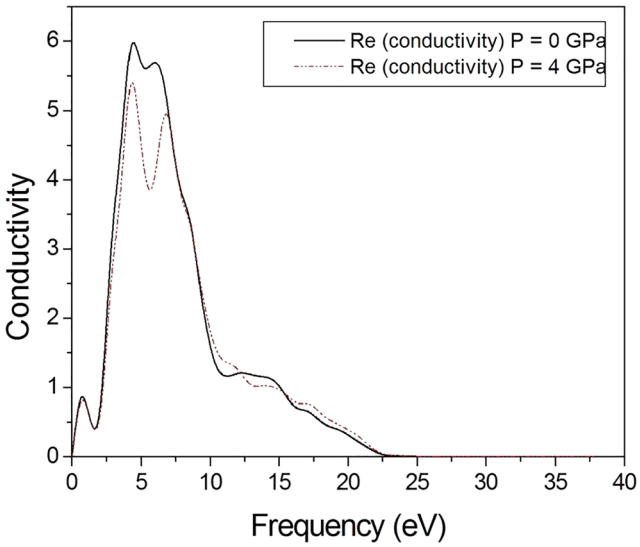

Fig. 7 Optical conductivity spectrum for zinc blende MnTe at zero pressure and under 4 GPa pressure

The energy loss of fast electrons traversing in a semiconductor material is described by the energy loss function. For that purpose, the electron energy loss function for zinc blende MnTe at zero pressure and under 4 GPa pressure has been computed. Our results are shown in Fig. 8. In these spectra, one can note peaks that represent the

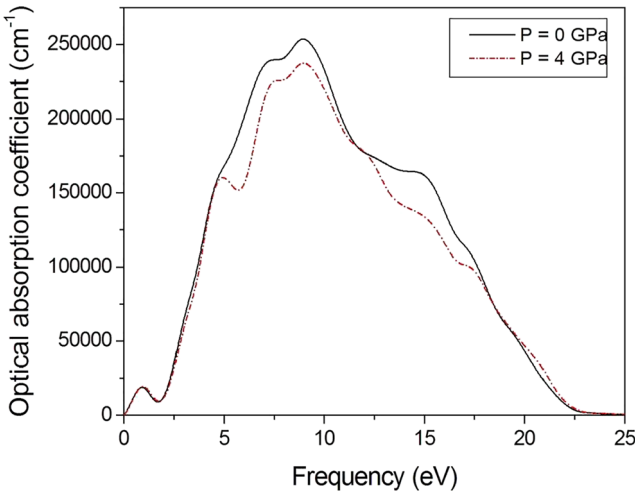

Fig. 6 Optical absorption coefficient spectrum for zinc blende MnTe at zero pressure and under 4 GPa pressure

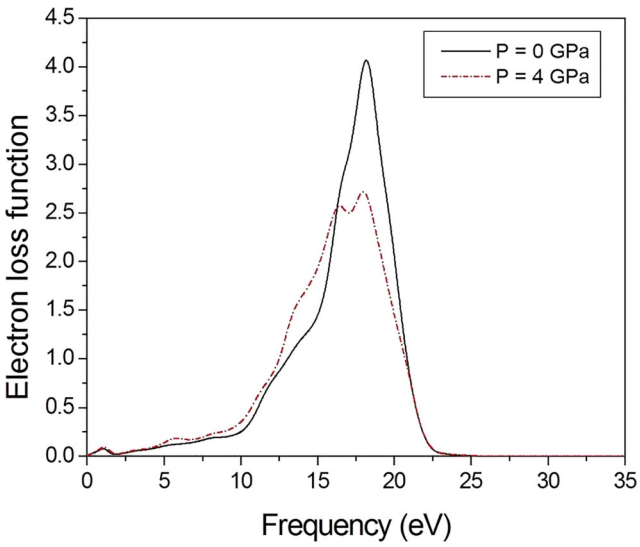

Fig. 8 Electron energy loss spectrum for zinc blende MnTe at zero pressure and under 4 GPa pressure

characteristic associated with the plasma resonance. The plasma frequency corresponds to that plasma. When pressure is applied, the plasma frequency is slightly shifted towards smaller energies and the maximum of the peak is reduced followed by a change in the shape of the spectrum.

4 Conclusion

In summary, the structural and mechanical properties and optical spectra of the MnTe semiconductor compound were investigated using the pseudopotential plane-wave method in the LDA approach. The crystal structure of MnTe was a zinc blende. Features such as lattice constant, bulk modulus and its pressure derivative, elastic constants and some of their related parameters, optical absorption coefficient, real and imaginary parts of the dielectric function, optical conductivity, and electron loss function were studied, and their dependence on hydrostatic pressure was analyzed and discussed. Our results at zero pressure were found to be in reasonably good agreement with the data reported in the literature. The mechanical behavior was examined in terms of ductility and brittleness, indicating that the material of interest behaves in a ductile manner. The generalized elastic stability criteria suggested that zinc blende MnTe is mechanically stable in the pressure range of 0–4 GPa. The influence of pressure was found to affect significantly all the properties of interest, thus giving new physical parameters.

References

1. Weidemann, R., Gumlich, H.-E., Kupsch, M., Middelmann, H.-U., Becker, U.: Phys. Rev. B **45**, 1172 (1992)
2. Abramof, E., Faschinger, W., Sitter, H., Pesek, A.: Appl. Phys. Lett. **64**, 49 (1994)
3. Gonzalez Szwacki, N., Przeździecka, E., Dynowska, E., Bogusawski, P., Kossut, J.: Acta Phys. A **106**, 233 (2004)
4. Djemia, P., Roussigné, Y., Stashkevich, A., Szuszkiewicz, W., Gonzalez Szwacki, N., Dynowska, E., Janik, E., Kowalski, B.J., Karczewski, G., Boguslawski, P., Jouanne, M., Morhange, J.F.: Acta Phys. Pol., A **106**, 239 (2004)
5. Krause, M., Bechstedt, F.: J. Supercond. Nov. Magn. **26**, 1963 (2013)
6. Bouarissa, N., Gueddim, A., Siddiqui, S.A., Boucenna, M., Al-Hajry, A.: Superlattice. Microst. **72**, 319 (2014)
7. Ueda, Y., Sato, H., Taniguchi, M., Happo, N., Mihara, T., Namatame, H., Mizokawa, T., Fujimori, A.: J. Phys. Condens. Matter **6**, 8607 (1994)
8. Neitzel, U., Bärner, K.: Phys. Status Solidi B **129**, 707 (1985)
9. Allen, J.W., Lucovsky, G., Mikkelsen Jr., J.C.: Solid State Commun. **24**, 367 (1977)
10. Kunitomi, N., Hamaguchi, Y., Anzai, S.: J. Phys. **25**, 568 (1964)
11. Franzen, H., Sterner, C.: J. Solid State Chem. **25**, 227 (1978)
12. Ozawa, K., Anzai, S., Hamaguchi, Y.: Phys. Lett. **20**, 132 (1966)
13. Giebultowicz, T.M., Klosowski, P., Samarth, N., Luo, H., Furdyna, J.K., Rhyne, J.J.: Phys. Rev. B **48**, 12817 (1993)
14. Johnston, W.D., Sestrich, A.E.: J. Inorg. Nucl. Chem. **19**, 229 (1961)
15. Durbin, S.M., HanSungki, J., Kobayashi, O.M., Menke, D.R., Gunshor, R.L., Fu, Q., Pelekanos, N., Nurmikko, A.V., Li, D., Gosvales, J., Otsuka, N.: Appl. Phys. Lett. **55**, 2087 (1989)
16. Giebultowicz, T.M., Klosowski, P., Samarth, N., Luo, H., Furdyna, J.K., Rhyne, J.J.: Phys. Rev. B **48**, 12817 (1993)
17. Buschert, J.R., Peiris, F.C., Samarth, N., Luo, H., Furdyna, J.K.: Phys. Rev. B **49**, 4619 (1994)
18. Janik, E., Dynowska, E., Back, M.J., Leszczynski, M., Szuszkiewicz, W., Wojtowicz, T., Karczewski, G., Zakrzewski, A.K., Kossut, J.: Thin Solid Films **267**, 74 (1995)
19. Holzapfel, W.B.: Rep. Prog. Phys. **59**, 29 (1996)
20. Badding, J.V.: Annu. Rev. Mater. Sci. **28**, 631 (1998). and references cited therein
21. Ackland, G.J.: Rep. Prog. Phys. **64**, 483 (2001). and references therein
22. Yin, M.T., Cohen, M.L.: Phys. Rev. B **25**, 7403 (1982)
23. Payne, M.C., Teter, M.P., Allan, D.C., Arias, T.A., Joannopoulos, J.D.: Rev. Mod. Phys. **64**, 1045 (1992)
24. Bouarissa, N.: Mater. Chem. Phys. **65**, 107 (2000)
25. Bouarissa, N.: Europ. Phys. J. B **26**, 153 (2002)
26. Bouarissa, N.: Phys. B **406**, 2583 (2011)
27. Daoud, S., Bioud, N., Bouarissa, N.: Mater. Sci. Semicond. Process. **31**, 124 (2015)
28. Clark, S.J., Segall, M.D., Pickard, C.J., Hasnip, P.J., Probert, M.J., Refson, K., Payne, M.C.: Z. Krist. **220**, 567 (2005)
29. Vanderbilt, D.: Phys. Rev. B **41**, 7892 (1990)
30. Ceperley, D.M., Alder, B.J.: Phys. Rev. Lett. **45**, 566 (1980)
31. Perdew, J.P., Zunger, A.: Phys. Rev. B **23**, 5048 (1981)
32. Monkhorst, H.J., Pack, J.D.: Phys. Rev. B **13**, 5188 (1976)
33. Fischer, T.H., Almlof, J.: J. Phys. Chem. **96**, 9768 (1992)
34. Milman, V., Warren, M.C.: J. Phys. Condens. Matter **13**, 241 (2001)
35. Reuss, A., Angew, Z.: Math. Mech. **9**, 49 (1929)
36. Voigt, W.: Lehrbuch der Kristallphysik. Teubner, Leipzig (1928)
37. Hill, R.: Proc. Phys. Soc. A **65**, 349 (1952)
38. Hill, R.: J. Mech. Phys. Solids **11**, 357 (1963)
39. Birch, F.: J. Geophys. Res. **57**, 227 (1952)
40. Birch, F.: J. Geophys. Res. **83**, 1257 (1978)
41. Pugh, S.F.: Philos. Mag. **45**, 823 (1954)
42. Gueddim, A., Zerroug, S., Bouarissa, N.: J. Lumin. **135**, 243 (2013)
43. Khan, M.A., Bouarissa, N.: Optik **124**, 5095 (2013)